Computer Methods in Applied Mechanics and Engineering 107 (1993) 209–223
North-Holland

CMA 409

Space-time finite element computation of compressible flows involving moving boundaries and interfaces*

S.K. Aliabadi and T.E. Tezduyar

Department of Aerospace Engineering and Mechanics, Army High-Performance Computing Research Center, and Supercomputer Institute, University of Minnesota, 1200 Washington Avenue South, Minneapolis, MN 55415, USA

Received 20 April 1992

The deformable-spatial-domain/stabilized-space-time (DSD/SST) formulation, introduced by Tezduyar et al. is applied to computation of viscous compressible flows involving moving boundaries and interfaces. The stabilization technique employed is a streamline-upwind/Petrov–Galerkin (SUPG) method, with a modified SUPG stabilization matrix. The stabilized finite element formulation of the governing equations is written over the space-time domain of the problem, and therefore the deformation of the spatial domain with respect to time is taken into account automatically. The frequency of remeshing is minimized to minimize the projection errors involved in remeshing and also to increase the parallelization potential of the computations. The implicit equation systems arising from the space-time finite element discretizations are solved iteratively. It is demonstrated that the combination of the SUPG stabilization and the space-time approach gives the capability of handling complicated compressible flow problems, including those with moving surfaces and shock-boundary layer interactions.

1. Introduction

The deformable-spatial-domain/stabilized-space-time (DSD/SST) formulation was first introduced, in the context of unsteady incompressible flows, by Tezduyar et al. [1,2] to compute flow problems involving moving boundaries and interfaces. The procedure was successfully applied to a variety of problems, including liquid drops, two-liquid flows, liquid-filled containers subjected to external motion, flows with drifting cylinders, and simple fluid-structure interaction problems such as oscillating cylinders and airfoils [2–4].

In the DSD/SST procedure, the stabilized finite element formulation corresponding to the governing equations of a flow problem is written over its space-time domain. This way, the

Correspondence to: Professor Tayfun E. Tezduyar, Minnesota Supercomputer Institute, 1200 Washington Avenue South, Minneapolis, MN 55415, USA.

* This research was sponsored by NASA-JSC under grant NAG 9-449 and by NSF under grant MSM-8796352. Partial support for this work has also come from the Army Research Office contract number DAAL03-89-C-0038 with the High Performance Computing Research Center at the University of Minnesota.

deformation of the spatial domain with respect to time is automatically taken into account. The motion of the free surfaces, interfaces and solid boundaries are accommodated by moving the boundary nodes, whereas the rest of the mesh can be moved in any way desired. We need to emphasize the difference between mesh moving and remeshing. In mesh moving, the nodal points move and the elements deform, but no new set of nodes or elements are generated. In remeshing, on the other hand, a new mesh with a new set of nodes and elements are generated, and the solution is projected from the old mesh to the new one. In our approach, we try to minimize the frequency of remeshing, because, by minimizing remeshing we not only reduce the projection errors involved in remeshing, but also increase the parallelization ease of the computations.

In the DSD/SST formulation, we use finite element interpolation functions which are piecewise bilinear and continuous in space, and piecewise linear and discontinuous in time. The discontinuity in time allows us to solve the fully discretized equations one space-time slab at a time, and this way the space-time computations can be carried out without generating unbearable computational costs, but also without loss of temporal accuracy. However, the computational cost associated with the space-time formulations based on interpolation functions linear in time can easily become quite high. Therefore, in our computations, the implicit equation systems arising from the space-time finite element discretizations are solved iteratively by using the GMRES [5] search technique with preconditioner. The preconditioners we employ are diagonal, nodal-block-diagonal or more sophisticated preconditioners such as the clustered element-by-element (CEBE) [6, 7] technique. The extensive numerical investigations involving oscillating cylinders and airfoils presented in [3, 4] were achieved by computations based on the CEBE preconditioners. The nearly optimum cluster size used in these computations was determined by numerical experimentation.

In this article, we extend the DSD/SST formulation to compressible flows involving moving boundaries and interfaces. The stabilization technique used for incompressible flows in [1, 2] is a Galerkin/least-squares (GLS) formulation. The GLS formulation includes two stabilization components: the streamline-upwind/Petrov–Galerkin (SUPG) stabilization and the pressure-stabilization. The SUPG stabilization prevents numerical oscillations that might be generated by the advection terms, and the pressure-stabilization prevents numerical oscillations that might be caused by certain combinations of interpolations functions for velocity and pressure. In our formulation for compressible flows, we use only the SUPG component, because, for the Mach number ranges we consider, we do not anticipate any need for pressure-stabilization. The SUPG stabilization for compressible Euler equations was first introduced by Tezduyar and Hughes [8, 9]. The journal version of [8] included some additional numerical examples [10]. The SUPG stabilization used in [8] was achieved in the context of conservation variables. Following that, similar stabilization techniques were employed, together with a shock-capturing term added to the formulation, in the context of entropy variables [11–13]. Recently, it was shown by Le Beau and Tezduyar [14] and Le Beau et al. [15] that SUPG formulation based on conservation variables, supplemented with a shock-capturing term, gives solutions which are not only just as good as but also barely distinguishable from those obtained with the entropy variables.

In this article, we introduce and employ a modified version of the SUPG stabilization technique given in [14, 15]. The motivation behind seeking a modified technique was our observation that the definition of the SUPG matrix used in [14, 15] sometimes resulted in

excessive numerical damping at high Mach numbers. This was, we believe, due to improper selection of the SUPG matrix with respect to the spatial coordinates and the shock-capturing term. The modified SUPG matrix takes into account the presence of the shock-capturing term and also the physical diffusion.

We apply the DSD/SST formulation to two numerical examples from compressible flows involving moving boundaries and interfaces. The first example is subsonic flow past a pitching airfoil; the second one is supersonic flow through an air intake. The second example was chosen to demonstrate the potential of the DSD/SST technique to handle complicated problems involving shock-boundary layer interactions and moving surfaces.

2. The governing equations

Let $\Omega_t \in \mathbb{R}^{n_{sd}}$ be the spatial domain at time $t \in (0, T)$, where n_{sd} is the number of space dimensions. Let Γ_t denote the boundary of Ω_t. We consider the conservation law form of the Navier–Stokes equations governing unsteady compressible flows with no source terms:

$$\frac{\partial \boldsymbol{U}}{\partial t} + \frac{\partial \boldsymbol{F}_i}{\partial x_i} - \frac{\partial \boldsymbol{E}_i}{\partial x_i} = 0 \quad \text{on } \Omega_t \quad \forall t \in (0, T), \tag{1}$$

where $\boldsymbol{U} = (\rho, \rho u_1, \ldots, \rho u_{n_{sd}}, \rho e)$ is the vector of conservation variables, $\boldsymbol{F}_i$ and $\boldsymbol{E}_i$ are, respectively, the Euler and viscous flux vectors defined as

$$\boldsymbol{F}_i = \begin{bmatrix} u_i \rho \\ u_i \rho u_1 + \delta_{i1} p \\ u_i \rho u_2 + \delta_{i2} p \\ u_i \rho u_3 + \delta_{i3} p \\ u_i (\rho e + p) \end{bmatrix} \tag{2}$$

and

$$\boldsymbol{E}_i = \begin{bmatrix} 0 \\ \tau_{i1} \\ \tau_{i2} \\ \tau_{i3} \\ -q_i + \tau_{ik} u_k \end{bmatrix}, \tag{3}$$

and repeated indices imply summation over the range of spatial dimension. Here ρ, $\boldsymbol{u}$ and p are the density, velocity and pressure, respectively, e is the total energy per unit mass, and δ_{ij} is the Kronecker delta. An equation of state relates the pressure to the other variables:

$$p = p(\rho, i), \tag{4}$$

where i is the internal energy per unit mass:

$$i = e - \tfrac{1}{2}|\boldsymbol{u}|^2. \tag{5}$$

For an ideal gas the equation of state becomes

$$p = (\gamma - 1)\rho i\,, \tag{6}$$

where γ is the ratio of the specific heats. The constitutive laws relating the viscous stress tensor τ_{ij} and heat flux vector q_i to the other variables are given as

$$\tau_{ij} = \mu\left(\left(\frac{\partial u_i}{\partial x_j} + \frac{\partial u_j}{\partial x_i}\right) - \frac{2}{3}\,\delta_{ij}\,\frac{\partial u_k}{\partial x_k}\right), \tag{7}$$

$$q_i = -\kappa\,\frac{\partial \theta}{\partial x_i}\,, \tag{8}$$

where θ is the temperature, and μ and κ are the coefficients of viscosity and thermal conductivity. The transport property coefficients μ and κ are assumed to be given based on Sutherland's formulae,

$$\mu = \mu_0\left(\frac{\theta}{\theta_0}\right)^{3/2}\frac{\theta_0 + 110}{\theta + 110}\,, \tag{9}$$

$$\kappa = \frac{\gamma R \mu}{(\gamma - 1)\mathrm{Pr}}\,, \tag{10}$$

where μ_0 is the viscosity at a reference temperature θ_0, R is the ideal gas constant, and Pr is the Prandtl number.

Alternatively, (1) can be written in a quasi-linear form as

$$\frac{\partial \boldsymbol{U}}{\partial t} + \boldsymbol{A}_i\,\frac{\partial \boldsymbol{U}}{\partial x_i} - \frac{\partial}{\partial x_i}\left(\boldsymbol{K}_{ij}\,\frac{\partial \boldsymbol{U}}{\partial x_j}\right) = 0 \quad \text{on } \Omega_t \quad \forall t \in (0, T)\,, \tag{11}$$

where

$$\boldsymbol{A}_i = \frac{\partial \boldsymbol{F}_i}{\partial \boldsymbol{U}} \tag{12}$$

and

$$\boldsymbol{K}_{ij}\,\frac{\partial \boldsymbol{U}}{\partial x_j} = \boldsymbol{E}_i\,. \tag{13}$$

We assume that we also have an appropriate set of boundary and initial conditions associated with (11).

3. The deformable-spatial-domain/stabilized-space-time (DSD/SST) finite element formulation of compressible flows

In the DSD/SST formulation, we partition the time interval $(0, T)$ into subintervals $I_n = (t_n, t_{n+1})$, where t_n and t_{n+1} belong to an ordered series of time levels $0 = t_0 < t_1 < \cdots <$

$t_N = T$. Let Ω_t^h be the approximation to Ω_t in I_n, and let Γ_t^h be the boundary of Ω_t^h. Also let $\Omega_n = \Omega_{t_n}$ and $\Gamma_n = \Gamma_{t_n}$. We shall define the space-time slab Q_n as the domain enclosed by the surface Ω_n, Ω_{n+1} and P_n, where P_n is the surface described by the boundary Γ_t^h as t traverses I_n (see Fig. 1).

Finite element discretization of a space-time slab Q_n is achieved by dividing it into elements Q_n^e, $e = 1, 2, \ldots, (n_{el})_n$, where $(n_{el})_n$ is the number of elements in the space-time slab Q_n. Based on this discretization, for each space-time slab Q_n, we define the finite element interpolation function spaces $(S^h)_n$ and $(V^h)_n$ for the trial solutions and weighting functions, respectively. These function spaces are selected, with the Dirichlet boundary conditions in mind, as subsets of $[H^{1h}(Q_n)]^{n_{sd}+2}$, where $H^{1h}(Q_n)$ represents the finite dimensional function space over the space-time slab Q_n. Over the parent (element) domain, this space is formed by using first-order polynomials in space and time. Globally, the interpolation functions are continuous in space but discontinuous in time. However, for two-fluid flows, the solution and variational functions spaces for density and energy need to include functions which are discontinuous across the interface.

The DSD/SST formulation of (11) can be written as follows: start with

$$(U^h)_0^- = (U_0)^h , \tag{14}$$

where U_0 is the initial value of the vector U; sequentially for $Q_1, Q_2, \ldots, Q_{N-1}$, given $(U^h)_n^-$, find $U^h \in (S^h)_n$, such that $\forall W^h \in (V^h)_n$

$$\begin{aligned}
&\int_{Q_n} W^h \cdot \left(\frac{\partial U^h}{\partial t} + A_i \frac{\partial U^h}{\partial x_i} \right) dQ + \int_{Q_n} \left(\frac{\partial W^h}{\partial x_i} \right) \cdot \left(K_{ij} \frac{\partial U^h}{\partial x_j} \right) dQ \\
&- \int_{(P_n)_h} W^h \cdot H \, dP + \int_{\Omega} (W^h)_n^+ \cdot ((U^h)_n^+ - (U^h)_n^-) \, d\Omega \\
&+ \sum_{e=1}^{(n_{el})_n} \int_{Q_n^e} \tau \left(\frac{\partial W^h}{\partial t} + A_k^t \frac{\partial W^h}{\partial x_k} \right) \cdot \left(\frac{\partial U^h}{\partial t} + A_i \frac{\partial U^h}{\partial x_i} - \frac{\partial}{\partial x_i} \left(K_{ij} \frac{\partial U^h}{\partial x_j} \right) \right) dQ \\
&+ \sum_{e=1}^{(n_{el})_n} \int_{Q_n^e} \delta \left(\frac{\partial W^h}{\partial x_i} \right) \cdot \left(\frac{\partial U^h}{\partial x_i} \right) dQ = 0 .
\end{aligned} \tag{15}$$

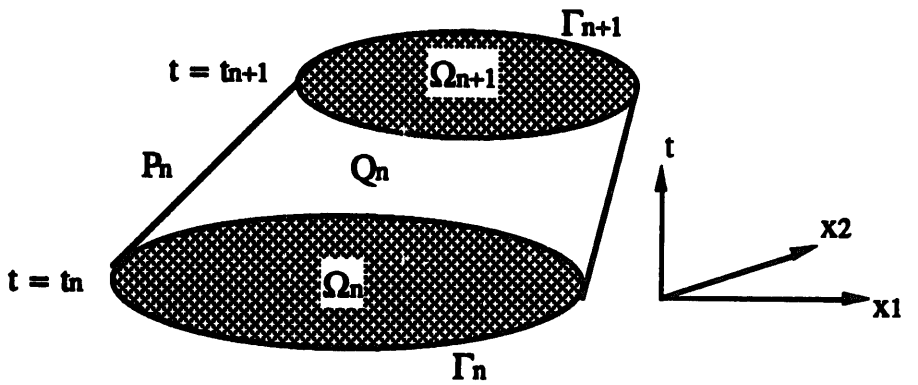

Fig. 1. The space-time slab for the DSD/SST formulation.

In the variational formulation given by (15), the following notation is used:

$$(U^h)_n^{\pm} = \lim_{\varepsilon \to 0} U^h(t_n \pm \varepsilon), \tag{16}$$

$$\int_{Q_n} (\cdots)\, dQ = \int_{I_n} \int_{\Omega} (\cdots)\, d\Omega\, dt, \tag{17}$$

$$\int_{P_n} (\cdots)\, dP = \int_{I_n} \int_{\Gamma} (\cdots)\, d\Gamma\, dt. \tag{18}$$

REMARK 1. In this formulation, the first four integrals represent the time-discontinuous Galerkin formulation of (11). The third integral accounts for the Neumann-type boundary conditions. The fourth integral enforces, weakly, the continuity of the conservation variables in time. The fifth and sixth integrals involving the matrix τ and coefficient δ are the SUPG and shock-capturing terms, respectively. These terms add numerical stability to the standard Galerkin variational formulation.

DEFINITION OF δ. The shock-capturing term used in this formulation is identical to the one introduced in [14, 15] for inviscid flows:

$$\delta = \left[\frac{A_i \dfrac{\partial U^h}{\partial x_i} \cdot \tilde{A}_0^{-1} A_j \dfrac{\partial U^h}{\partial x_j}}{\dfrac{\partial \xi_l}{\partial x_i} \dfrac{\partial U^h}{\partial x_i} \cdot \tilde{A}_0^{-1} \dfrac{\partial \xi_l}{\partial x_j} \dfrac{\partial U^h}{\partial x_j}} \right]^{1/2}, \tag{19}$$

where $\tilde{A}_0^{-1}$ is the Jacobian of the transformation from the conservation variables to the entropy variables, and ξ_l, $l = 1, 2, \ldots, n_{sd}$, are the components of the element (local) coordinate. The definition of $\tilde{A}_0$ and the details of the entropy variables are given in [11–13], and can also be found in [14, 15].

DEFINITION OF τ. The SUPG matrix

$$\tau = \max_{1 \le i \le n_{sd}} \alpha \frac{h_i}{\rho_i} I, \tag{20}$$

given in [14, 15], is a slightly modified version of the one introduced in [8–10]. Here I is the identity matrix, h_i is the element length in the x_i direction, α is a parameter controlling the stability and accuracy of the time-integration algorithm, and ρ_i is the spectral radius of A_i.

REMARK 2. Our experience shows that the definition of the matrix τ given by (20) sometimes results in excessive numerical damping at high Mach numbers. This, we believe, is due to improper selection of τ with respect to the spatial coordinates and the shock-capturing term.

The new SUPG matrix τ introduced in this paper is defined as

$$\tau = \max(0, \tau_a - \tau_\delta - \tau_d), \tag{21}$$

where τ_a is the stabilization matrix due to the advection terms, and τ_δ and τ_d are the matrices subtracted from τ_a to account for the presence of the shock-capturing term and the physical diffusion. These matrices are defined as

$$\tau_a = \frac{\max(\alpha h_i |\beta_i|)}{c + |\boldsymbol{u} \cdot \boldsymbol{\beta}|} \boldsymbol{I} \quad \text{(no sum)}, \tag{22}$$

$$\tau_\delta = \frac{\delta}{(c + |\boldsymbol{u} \cdot \boldsymbol{\beta}|)^2} \boldsymbol{I}, \tag{23}$$

$$\tau_d = \frac{(\beta_1^2 \operatorname{diag} \boldsymbol{K}_{11} + \beta_2^2 \operatorname{diag} \boldsymbol{K}_{22} + \beta_3^2 \operatorname{diag} \boldsymbol{K}_{33})}{(c + |\boldsymbol{u} \cdot \boldsymbol{\beta}|)^2}, \tag{24}$$

where c is the acoustic speed,

$$\boldsymbol{\beta} = \frac{\nabla \|\boldsymbol{U}\|_*^2}{\|\nabla \|\boldsymbol{U}\|_*^2\|_2}, \tag{25}$$

and

$$\|\cdot\|_* = \|\cdot\|_2 \quad \text{or} \quad \|\cdot\|_{\tilde{A}_0^{-1}}. \tag{26}$$

In regions where the solution is smooth, the shock capturing coefficient is very small. As a result, τ_δ is very small compared to τ_a, and the shock capturing term is inactive in these regions. On the other hand, when τ goes to zero, the SUPG term drops out from the formulation and the shock capturing term is the only stabilization term left. This most likely happens in regions where the solution is sharp, i.e., in the presence of shocks or boundary layers.

4. Numerical examples

In this section, we present two numerical examples involving computation of two-dimensional air flow (with $\Pr = 0.72$, $R = 287\ \text{J/(kg K)}$, $\gamma = 1.4$, $\mu_0 = 1.8 \times 10^{-5}\ \text{kg/(m s)}$ and $\theta_0 = 300\ \text{K}$). The finite element interpolation functions employed are bilinear in space and linear in time. The implicit equation systems arising from the space-time finite element discretization are solved iteratively by using a nodal-block-diagonal preconditioner with the GMRES [5] search technique.

4.1. Mach 0.2 flow past a pitching airfoil at Reynolds number 1000

This problem is the compressible flow version of the one considered by Mittal and Tezduyar [4]; it involves Mach 0.2 (close to incompressible) flow past a pitching NACA 0012 airfoil. The Reynolds number based on the free-stream velocity and the airfoil chord length is 1000. The coordinates of the half-chord center of the airfoil are (0, 0). The computational domain, which spans the area $-3 \leq x_1 \leq 10$, $-3 \leq x_2 \leq 3$, is discretized by employing 4564 elements and 4694

nodes. At the inflow and top and bottom boundaries, density, velocity and temperature are prescribed to be 1.225 kg/m^3, (69.4, 0.0) m/s and 300 K, respectively. At the outflow boundary, zero stress and zero heat flux conditions are imposed. On the airfoil, no slip and zero heat flux conditions are imposed. At each time step, approximately 38,000 equations are solved simultaneously. The initial condition consists of the steady-state solution at 10° angle of attack. Then, the airfoil is forced to pitch about its half-chord point with the prescribed angular motion

$$\varphi(t) = \frac{\varphi_{\max} + \varphi_{\min}}{2} - \frac{\varphi_{\max} - \varphi_{\min}}{2} \cos(2\pi t), \tag{27}$$

where $\varphi_{\min}$ and $\varphi_{\max}$ are 10° and 30°, respectively.

Figure 2 shows the Mach number at various instants during the first half period of the airfoil motion. Time histories of the lift, drag and moment coefficients are displayed in Fig. 3. The minimum values of these three quantities (corresponding to the more incompressible phase) compares well with those reported in [4], whereas the maximum values differ by 5–10%, and this difference can be attributed to compressibility. Figure 4 shows the full finite element mesh and close-up views of the mesh corresponding to the two extreme positions of the airfoil. From this figure it can be seen that the mesh around the airfoil undergoes rigid-body motion with the airfoil as it pitches. This is a desirable feature as it eliminates the mesh deformation near the airfoil. The mesh moving strategy used for this problem is such that the initial mesh remains topologically unchanged throughout the simulation. This eliminates the projection errors associated with remeshing and also increases the parallelization ease of the computations.

4.2. *Mach 1.4 air intake*

This problem was chosen to demonstrate the potential of the DSD/SST formulation to model intricate flows involving interactions between boundary layers, shocks and moving surfaces. This type of flow is encountered in the air intake of jet engines with adjustable spool. The efficiency of these engines at supersonic speeds are highly related to the adaptation of the outstanding shock. The shock adaptation is achieved by moving the spool back and forth until the desired configuration is obtained. In this problem, we consider the internal flow through an air intake with geometry shown in Fig. 5. The free-stream Mach number is 1.4, and the Reynolds number based on H (see Fig. 5) is 7500. Due to the assumed symmetry of the problem, only half of the domain is considered. At the inflow boundary (line 1–2), density, velocity and temperature are prescribed to be 1.225 kg/m^3, (486.0, 0.0) m/s and 300 K, respectively. At the outflow boundary (line 5–6), zero stress and zero heat flux conditions are imposed. On the solid surfaces, no slip and zero heat flux conditions are imposed. On the boundaries 2–3, 4–5, 6–7 and 8–1, the vertical component of the velocity is set to zero. The origin of the coordinate frame is located at half-way between points 3 and 8. The computational domain, which covers the area $-0.25 \leq x_1 \leq 0.85$, $-0.125 \leq x_2 \leq 0.125$, is discretized by employing 12,000 elements and 12,236 nodes. At each time step, approximately 100,000 equations are solved simultaneously. The initial condition is the steady-state solution corresponding to the configuration given in Fig. 5. At this initial configuration, two oblique sharp layers are formed at the inlet and are reflected to the boundary layers inside the domain; this

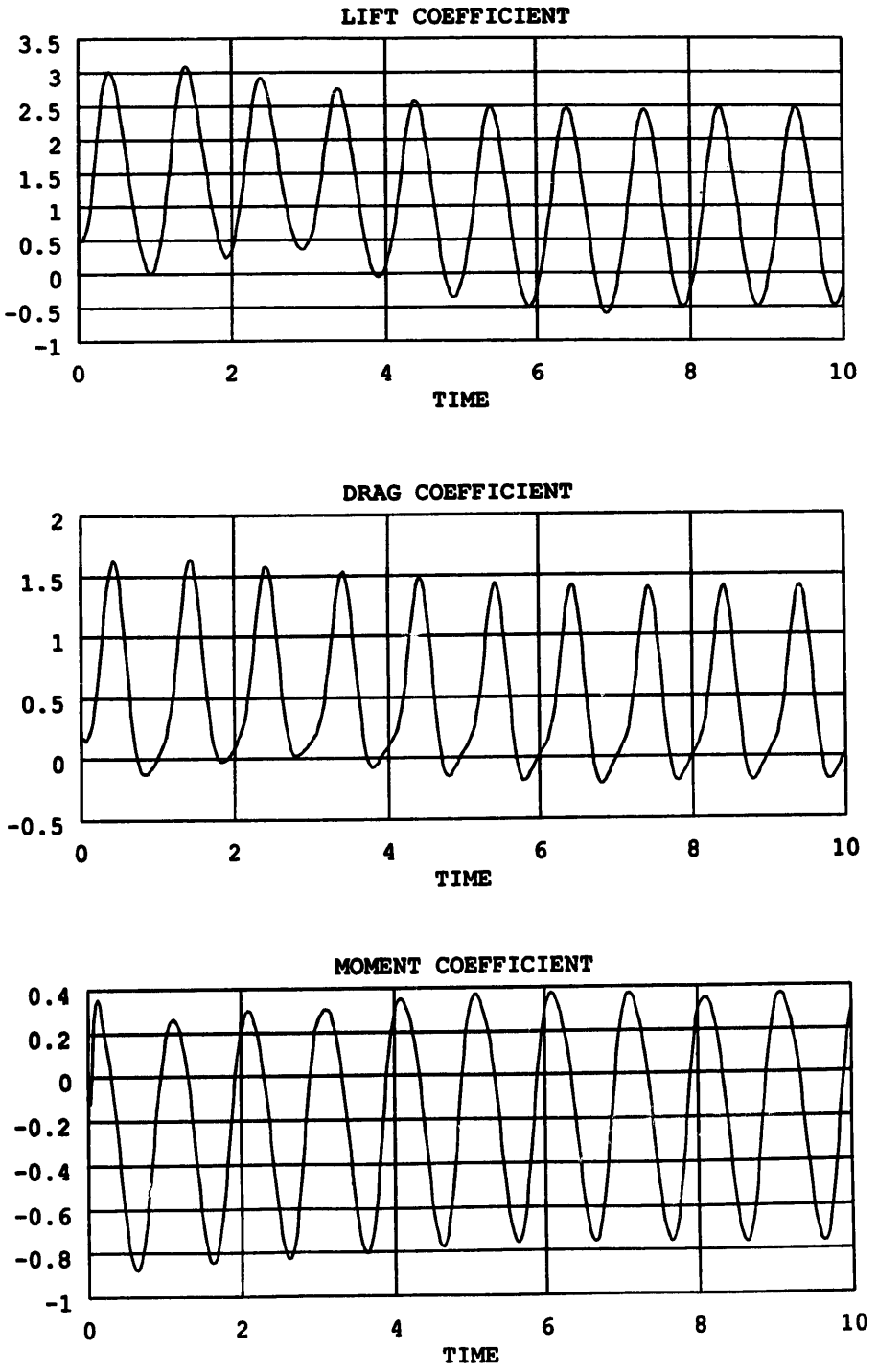

Fig. 3. Mach 0.2 flow past a pitching airfoil at Reynolds number 1000: time histories of the lift, drag and moment coefficients.

results in a complicated flow pattern. At time $t = 0$, the lower semi-wedge starts to move with the following equation of motion:

$$\Delta x_1(t) = -L \sin(\pi t) , \tag{28}$$

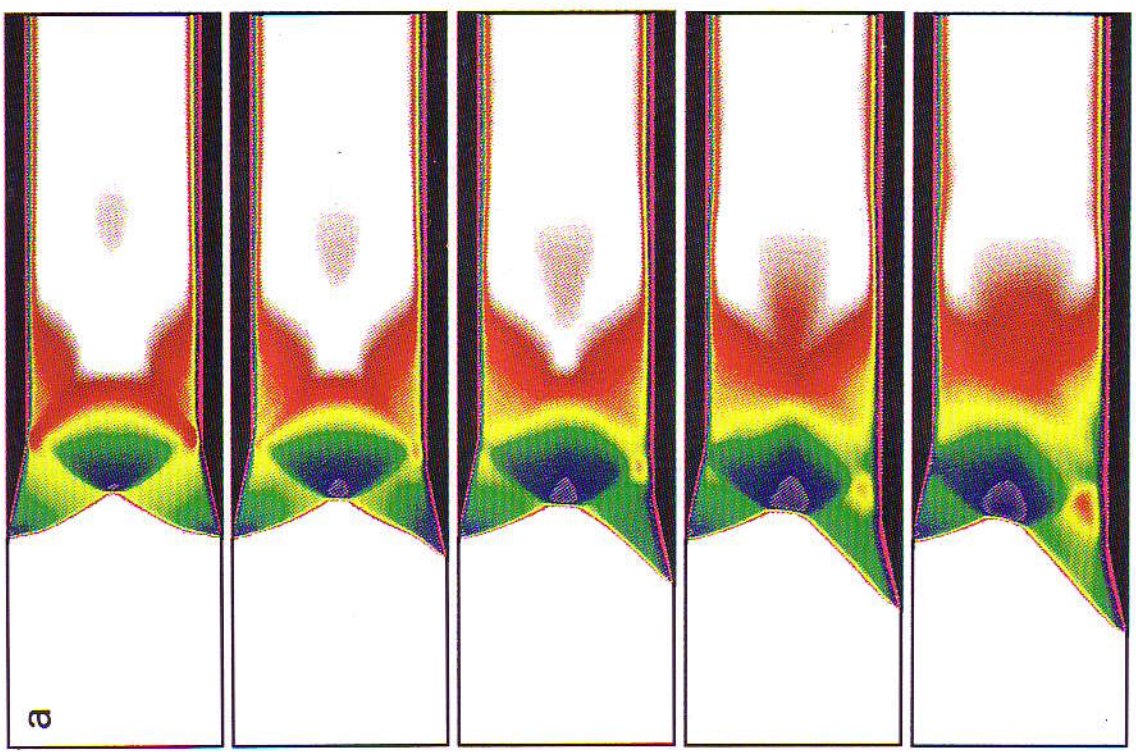

Fig. 6a. Mach 1.4 air intake: Mach number at various instants in the time interval [0.0, 0.2].

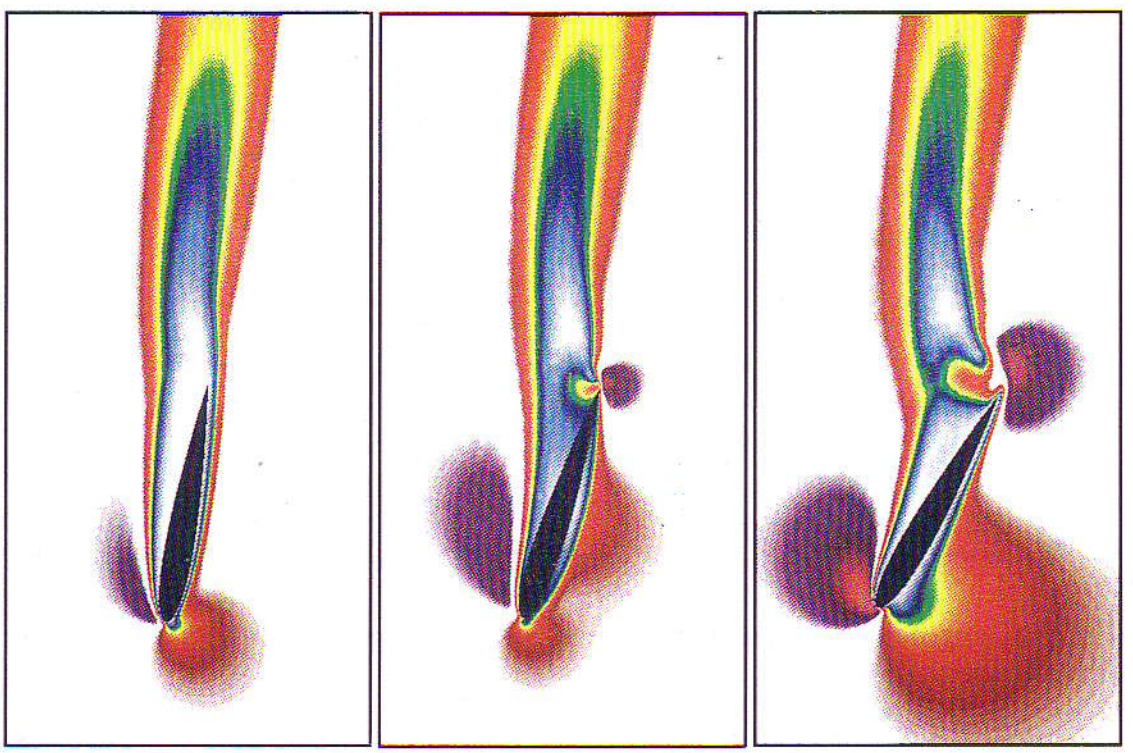

Fig. 2. Mach 0.2 flow past a pitching airfoil at Reynolds number 1000: Mach number at various instants during the first half period of the airfoil motion.

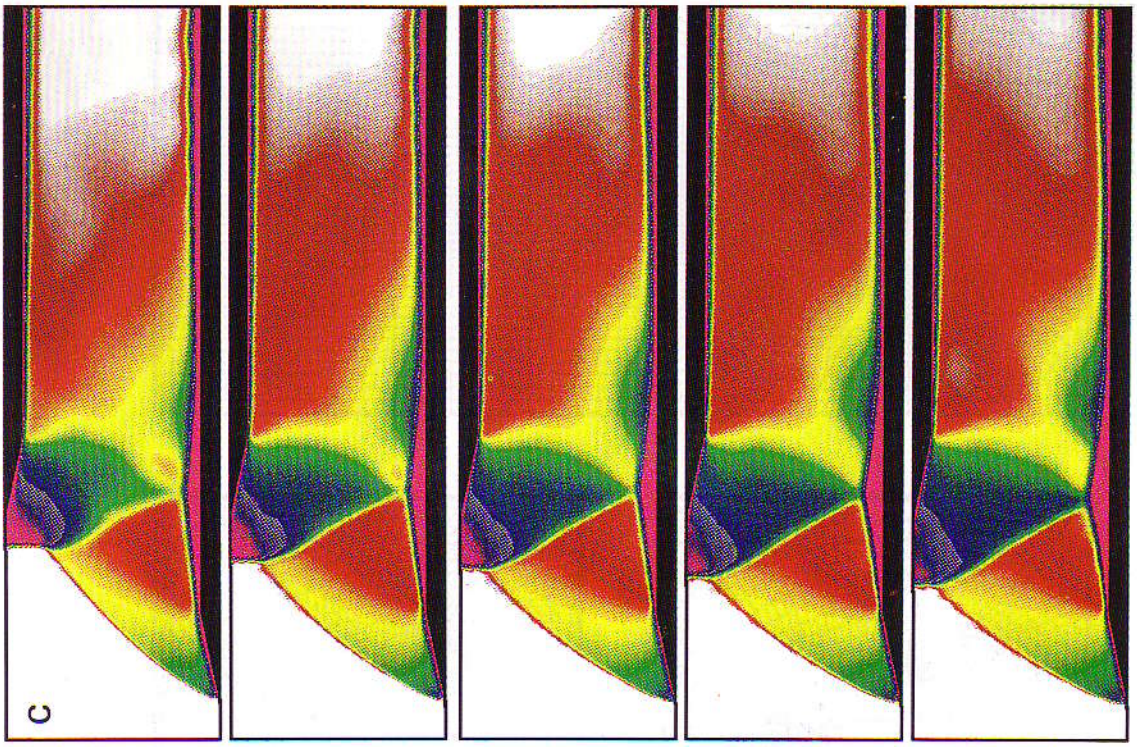

Fig. 6c. Mach 1.4 air intake: Mach number at various instants in the time interval [0.5, 0.7].

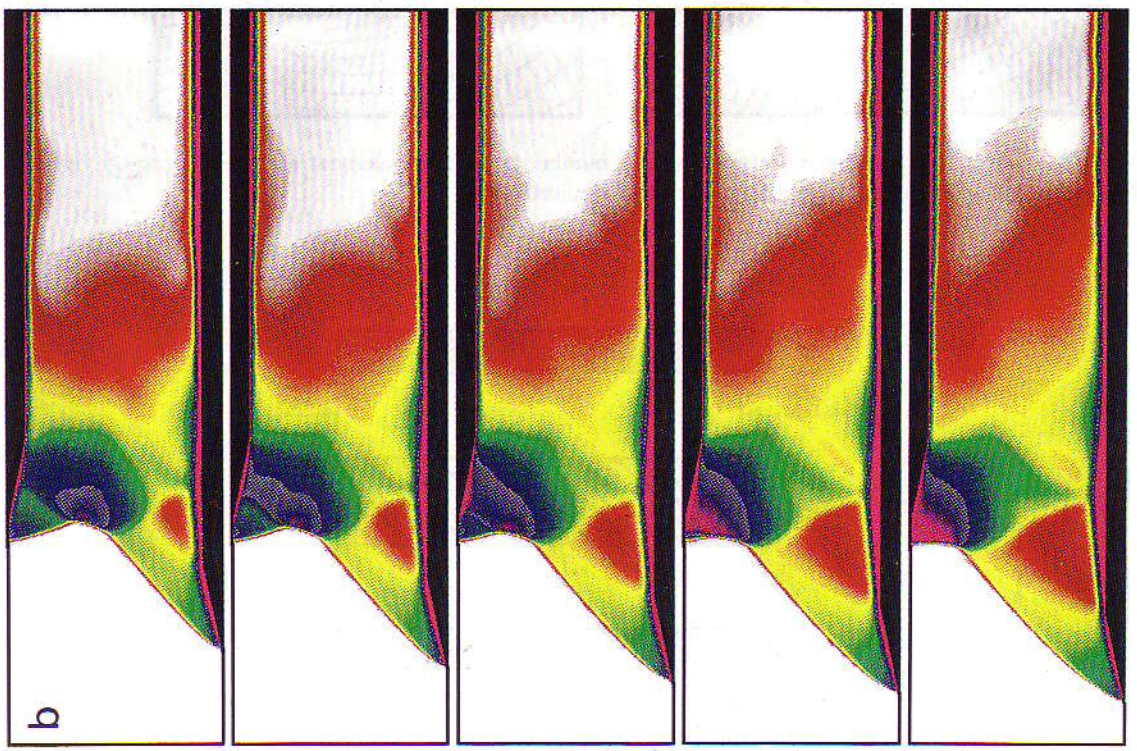

Fig. 6b. Mach 1.4 air intake: Mach number at various instants in the time interval [0.25, 0.45].

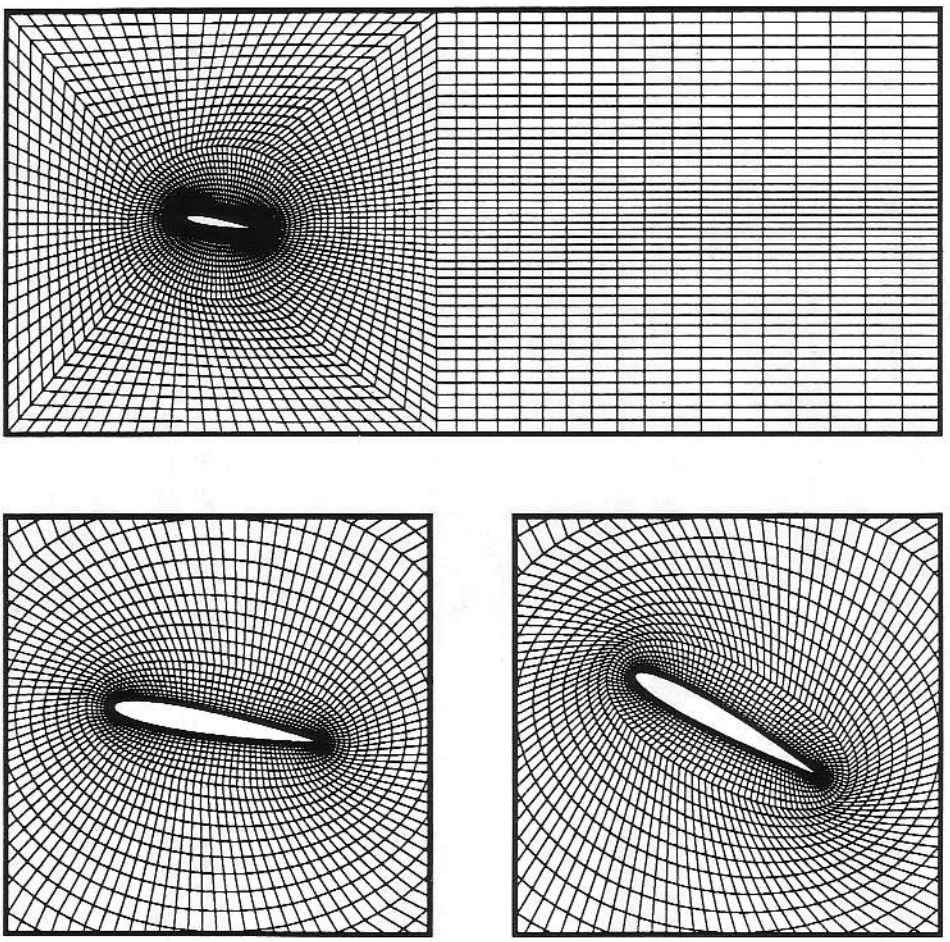

Fig. 4. Mach 0.2 flow past a pitching airfoil at Reynolds number 1000: finite element mesh and close-up views of the mesh corresponding to the two extreme positions of the airfoil.

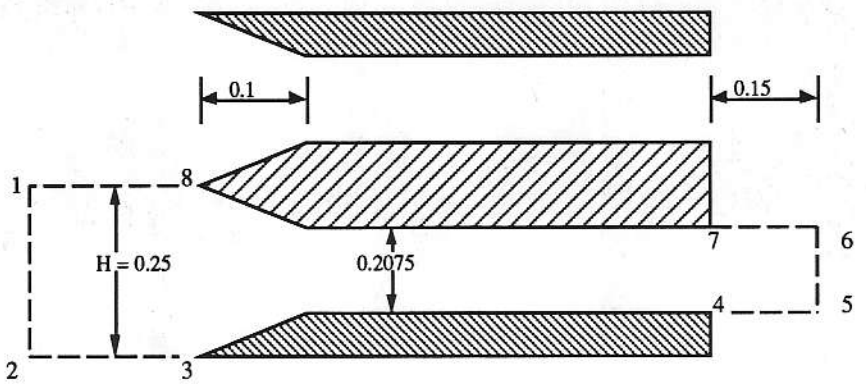

Fig. 5. Problem geometry for Mach 1.4 air intake.

where $L(=0.2)$ is the maximum range of the motion. The motion continues until Δx_1 reaches -0.2 (at $t = 0.5$).

Figure 6 shows a sequence of frames depicting the Mach number for the time interval $[0.0, 0.7]$. The shock at the leading edge of the lower surface is always attached and its interaction with the moving wedge results in a detached shock at the upper surface. This detached shock is reflected down where it interacts with the boundary layers and causes

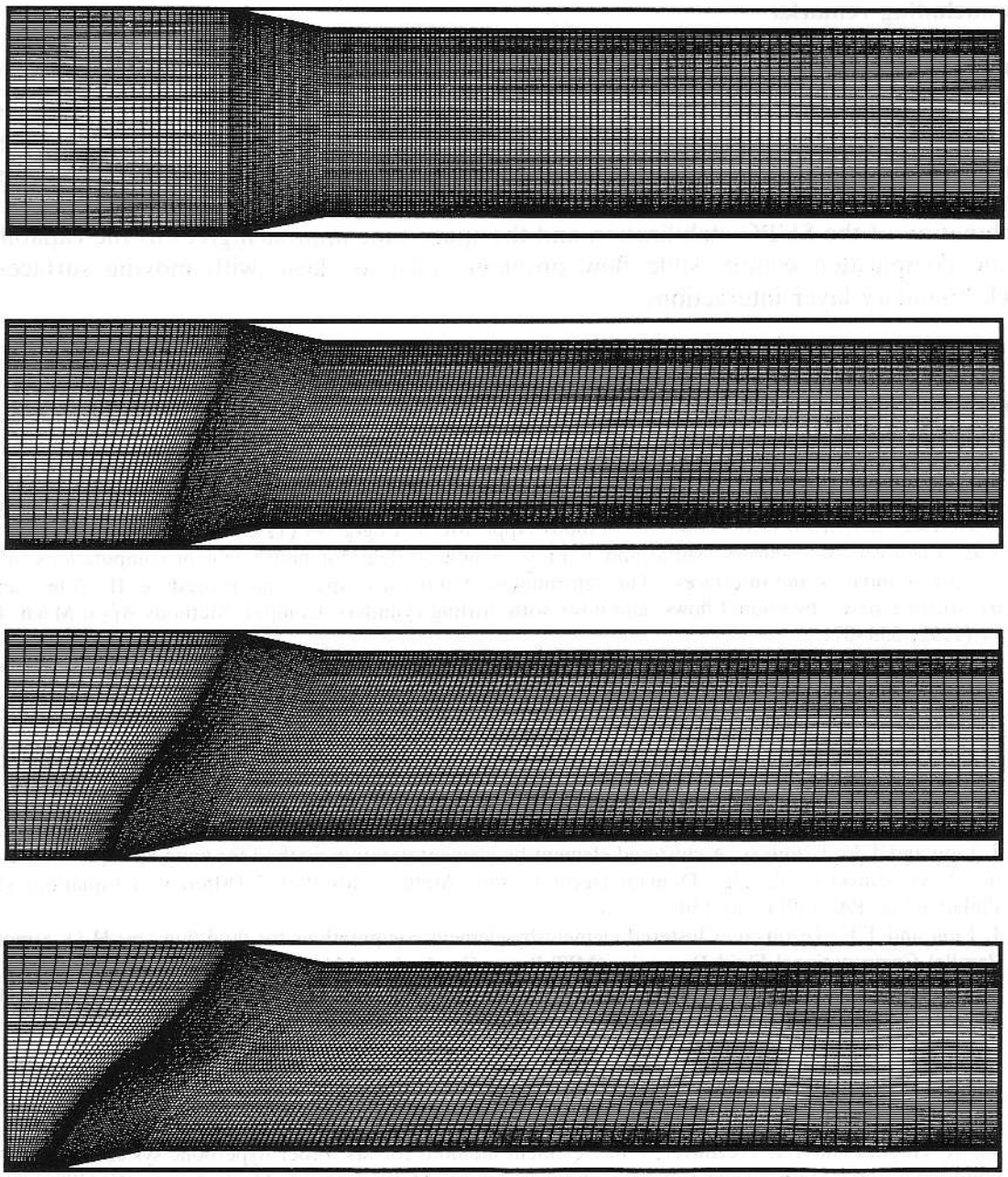

Fig. 7. Mach 1.4 air intake: finite element mesh at various instants in the time interval $[0.0, 0.5]$.

separation. Figure 7 shows the finite element mesh at various instants in the time interval [0.0, 0.5]. Since the deformation of the mesh is not large, we avoid remeshing by preserving the initial mesh topology. At each time step, the coordinates of the nodal points are changed, but the connectivity between the nodes remains unchanged.

5. Concluding remarks

We have extended the deformable-spatial-domain/stabilized-space-time (DSD/SST) formulation to computation of compressible flows involving moving boundaries and interfaces. In this formulation, a SUPG-stabilized finite element formulation is written over the space-time domain. A modified SUPG stabilization based on a new SUPG stabilization matrix was also introduced and employed with the space-time formulation. We demonstrated that the combination of the SUPG stabilization and the space-time approach gives us the capability to handle complicated compressible flow problems such as those with moving surfaces and shock-boundary layer interactions.

References

[1] T.E. Tezduyar, M. Behr and J. Liou, A new strategy for finite element computations involving moving boundaries and interfaces – The deforming-spatial-domain/space-time procedure: I. The concept and the preliminary numerical tests, Comput. Methods Appl. Mech. Engrg. 94 (1992) 339–351.

[2] T.E. Tezduyar, M. Behr, S. Mittal and J. Liou, A new strategy for finite element computations involving moving boundaries and interfaces – The deforming-spatial-domain/space-time procedure: II. Computation of free-surface flows, two-liquid flows, and flows with drifting cylinders, Comput. Methods Appl. Mech. Engrg. 94 (1992) 353–371.

[3] S. Mittal, A. Ratner, D. Hastreiter and T.E. Tezduyar, Space-time finite element computation of incompressible flows with emphasis on flows involving oscillating cylinders, Internat. Video J. Engrg. Res. 1 (1991) 83–86.

[4] S. Mittal and T.E. Tezduyar, A finite element study of incompressible flows past oscillating cylinders and airfoils, Internat. J. Numer. Methods Fluids 15 (1992) 1073–1118.

[5] Y. Saad, A flexible inner-outer preconditioned GMRES algorithm, University of Minnesota Supercomputer Institute Research Report 91/279, 1991.

[6] J. Liou and T.E. Tezduyar, A clustered element-by-element iteration method for finite element computations, in: R. Glowinski et al. eds., Domain Decomposition Methods for Partial Differential Equations (SIAM, Philadelphia, PA, 1991) 140–150.

[7] J. Liou and T.E. Tezduyar, Clustered element-by-element computations for fluid flow, in: H.D. Simon, ed., Parallel Computational Fluid Dynamics (MIT Press, Cambridge, MA, 1992) Chapter 9, pp. 167–187.

[8] T.E. Tezduyar and T.J.R. Hughes, Development of time-accurate finite element techniques for first-order hyperbolic systems with particular emphasis on the compressible Euler equations, report prepared under NASA-Ames University consortium Interchange No. NCA2-OR745-104, 1982.

[9] T.E. Tezduyar and T.J.R. Hughes, Finite element formulations for convection dominated flows with particular emphasis on the compressible Euler equations, AIAA Paper 83-0125, Proc. AIAA 21st Aerospace Sciences Meeting, Reno, NV, 1983.

[10] T.J.R. Hughes and T.E. Tezduyar, Finite element methods for first-order hyperbolic systems with particular emphasis on the compressible Euler equations, Comput. Methods Appl. Mech. Engrg. 45 (1984) 217–284.

[11] T.J.R. Hughes, L.P. Franca and M. Mallet, A new finite element formulation for computational fluid

dynamics: I. Symmetric forms of the compressible Euler and Navier–Stokes equations and the second law of thermodynamics, Comput. Methods Appl. Mech. Engrg. 54 (1986) 223–234.

[12] T.J.R. Hughes and M. Mallet, A new finite element formulation for computational fluid dynamics: III. The generalized streamline operator for multidimensional advective-diffusive systems, Comput. Methods Appl. Mech. Engrg. 58 (1986) 305–328.

[13] T.J.R. Hughes and M. Mallet, A new finite element formulation for computational fluid dynamics: IV. A discontinuity-capturing operator for multidimensional advective-diffusive systems, Comput. Methods Appl. Mech. Engrg. 58 (1986) 329–339.

[14] G.J. Le Beau and T.E. Tezduyar, Finite element computation of compressible flows with the SUPG formulation, in: M.N. Dhaubhadel, M.S. Engelman and J.N. Reddy, eds., Advances in Finite Element Analysis in Fluid Dynamics, FED-Vol. 123 (ASME, New York, 1991) 21–27.

[15] G.J. Le Beau, S.E. Ray, S.K. Aliabadi and T.E. Tezduyar, SUPG finite element computation of compressible flows with the entropy and conservation variables formulations, Comput. Methods Appl. Mech. Engrg. 104 (1993) 397–422.